MMA Memo 260
A Comparison of Zoom Arrays with Circular and Spiral Symmetry

John Conway
Onsala Space Observatory
S-43992, Sweden
email: jconway@oso.chalmers.se

April 12th, 1999

Abstract

There are advantages in making the intermediate arrays of the MMA/LSA which fill the 3km plain so-called 'zoom' arrays. In such arrays the antenna pads are arranged according to a scale-free self-similar distribution. By moving antennas from inner pads to outer ones the array gradually expands keeping a self-similar uv coverage. So far two types of zoom array have been proposed, one based on a definite shape, a three-armed logarithmic spiral (Conway 1998), and another assuming a circularly symmetric inverse-square law density of pads (Webster 1998). In this memo we make a first comparison of these two geometries. In the arrays tested we find small but significant advantages of the spiral geometry over the circularly symmetric ones; both in terms of uv coverage and how well the geometry stays self-similar as the array zooms. Although better untested circularly symmetric configurations may exist the advantages we see for the spiral appear to be intrinsic; coming fundamentally from its three-fold symmetry and the 'open' nature of this pattern. Despite these small differences we argue that both circular and spiral zoom arrays have better capabilities than the series of set array configurations that have dominated array configuration planning up to now.

1 Introduction

Most studies of the MMA/LSA antenna configurations have assumed that there will be a small number of set arrays of different sizes like the VLA. A radically different approach is to abandon the idea of set configurations entirely. In this approach there is a distribution of pads which are partially occupied at one time and antennas are continously being moved from the innermost occupied pads to outer pads. The first MMA/LSA design which allowed such operation was given by Conway (1998), based on a logarithmic spiral geometry. Subsequently Webster (1998) presented a circularly symmetric concept with similar properties.

There are a number of advantages to zoom arrays. Such arrays have no large jumps in resolution as we get in the case of set configurations. Furthermore we can arrange observations at different frequencies in different line transitions to have almost exactly the same uv coverage and resolution

- which is clearly important for line-ratio studies. Choosing such self-similar pad distributions also naturally leads to maximum pad sharing between configurations, reducing infrastructure costs. Finally - rather than having short intense periods of reconfiguration requiring a significant temporary workforce, in the zoom array concept a crew of 2 or 3 people can be permanently employed to carry out the constant reconfiguration.

2 Self-Similar Spiral Arrays

Although a number of authors have suggested the principle of continuously adjustable arrays (e.g. Viallefond 1998) the first detailed design for such an array for the MMA was proposed by Conway (1998). This design was based on self-similar spiral geometries. It was argued that it was natural to base the zoom array on some semi-regular self-similar geometry which would then maximise pad and other infrastructure sharing between different sized antenna configurations. It was argued that the spiral was an optimum compromise between 'open' Y-shaped configurations and closed configurations of nested loops (usually circles or triangles). The former naturally provide continuous scaling as telescopes are moved out along the arms - but have poor 2-dimensional snapshot uv coverage. In contrast nested loop geometries have good snapshot coverages but are only perfectly scaled for ratios equal to that of the nested loops.

It is interesting to note in passing that the excellent properties of spiral patterns are well known within standard antenna theory (V. Belitsky, private communication). Such spiral antennas give excellent beam patterns which are self-similar with frequency; and are therefore used for wide-bandwidth planar antennas on aircraft and in other applications.

Conway (1998) presented a design for the LSA/MMA based on a 3-armed spiral in which each arm turned by approximately 1.5 turns while the radius increased by a factor of 8 which was shown to have excellent snapshot uv coverage characteristics. In particular the distribution of the uv points was close to gaussian giving a naturally weighted main beam which was also gaussian. This was argued to be a desirable property, since an estimate of the source brightness after being convolved with a gaussian is precisely what the astronomer desires. Such a natural beam shape also gives the optimum map signal to noise - any other distribution requires in effect non-uniform weighting of the data - reducing the signal to noise.

The uv-coverage and zoom properties of the spiral array proposed by Conway (1998) were shown to be excellent with the resolution being very finely adjustable by moving a single telescope per arm (see Figure 4 of Conway (1998)). By moving only one third of the total number of antennas the resolution could be changed by a factor of two. With two pads per antenna the array could fully cover the range in baseline required by the intermediate arrays from a smallest array with minimum baseline 400m to the largest with 3000m maximum baseline (see Figure 5 of Conway(1998)). Therefore in contrast to the claim of Webster(1998) the design did not possess a small zoom range. In terms of the nomenclature of Webster (1998) the zoom range was $Z = 8$ not $Z = \sqrt{8}$ as claimed (the error arose from confusing the range of radii sampled by the pads, which was $R_s = 64$, with the range of radii covered by the telescopes at any given time, $R = 8$).

3 Circularly Symmetric Zoom Arrays

Webster (1998) discussed a general class of zoom array, based on a semi-analytical approach in which the array was modelled by a smoothly varying function $\rho(r)$ characterising the density of pads per unit area, and the antennas were assumed distributed in a perfectly circularly symmetric fashion. All pads between a certain inner radius and an outer radius are assumed to be occupied at one time (Nb Webster (1999), relaxes this assumption). If the inner and outer occupied radius is varied as the array is zoomed then it can be shown that the only distribution law which gives a self-similar distribution (with inner and outer radius having a fixed ratio) while conserving the number of telescopes has $\rho(r) \propto r^{-2}$. Assuming this continuous density distribution function and perfect circular symmetry, the radial profiles of the circularly symmetric natural dirty beams were then calculated analytically via Hankel transforms. These beam shapes were shown to be good provided the ratio of inner to outer filled radius was sufficiently large (i.e. greater than about four).

4 Comparison of UV Coverages

It is interesting to compare directly the properties of the spiral and circularly symmetric zoom array designs for realistic numbers of elements. In particular the results of Webster(1998) were derived analytically assuming continuous antenna density distributions - and therefore only strictly apply in the limit of an infinite number of antennas. Furthermore it is interesting to compare designs based respectively on triangular and circular symmetry. For antennas *on* a fixed perimeter it has been found (Keto 1997) that triangular symmetry gives better uv coverages and beam patterns than circular symmetry. It is interesting to see if the same is true for 'filled' configurations in which the antennas all lie *within* a circularly or triangularly symmetric outer perimeter.

We have simulated zenith snapshot uv coverages and dirty beams (see Figs 1,2 and 3) for different arrays of 48 (or in one case 49) antennas which all cover a range of radii from the array centre of 10; giving a large instantaneously sampled range of baseline length (approximately 30-40). Such a range in radius also allows the number of pads required to be minimised. If two pads per antenna are assumed then it is possible to zoom in a self-similar fashion over a range of baseline length of 10; from the largest array having a maximum baseline of approximately 3000m which fills the 3km plain to the smallest which has maximum baseline of 300m. The latter array would then smoothly connect with the most compact 'close-pack' array.

4.1 Criteria

The exact criteria to use in evaluating the quality of a uv coverage/dirty beam pattern is not clear; although imaging simulations clearly show that that the exact distribution of antennas does strongly effect imaging quality (see Kogan 1999).

Kogan(1998) uses as a metric for an array's imaging quality the size of the largest sidelobe within a given radius from the centre of the dirty beam. This has the great advantage that it is a conveniently computed quantity. However it can be argued that this metric has several disadvantages. First it depends on one largest value of the beam and not its average fluctuations. Furthermore algorithms which optimise the dirty beam within a given radius (e.g Kogan 1998) must to some extent do this the expense of increasing sidelobes outside of this radius (from Parseval's thereom). Although low sidelobe level are clearly a desirable property, other features such as range of baseline length sampled are also likely to be important and are not part of the criteria. Finally from considerations of imaging artifacts in CLEAN and other deconvolved images it is clear that uniformity of uv coverage in itself a very important criteria. It is well known that if there is a single significant hole in the uv coverage then the final deconvolved map will often contain large 'ripple' errors - yet the sidelobe level of the dirty beam may be comparable or only very slightly larger than a uniform uv coverage. Imaging quality appears to be a very non-linear function of the presence of small holes in the uv coverage.

Clearly detailed imaging simulations are needed to properly evaluate arrays. In the absence of such simulations we use in this memo as our criteria for evaluating zoom arrays the absence of large uv holes and a smooth distribution of points which approximates a random gaussian distribution. Of course such uv coverages also tend to have very low sidelobes, only slightly larger than those from arrays which explicitly minimise sidelobe level. For instance the peak sidelobe is around 0.1 for the *regular* 48 antenna spiral presented in Figs 1 and 2, which is the same as the peak sidelobe level for concentric-ring sidelobe-optimised array of 36 antennas (Kogan 1998).

4.2 Circular Random Arrays

In realising the zoom array geometry given by Webster (1998) for a finite number of elements some choice has to be made on how exactly to distribute the antennas in two dimensional space. The most straightforward way to interpret the required antenna density distribution $\rho(r) \propto r^{-2}$ (Webster 1998) is as a probability distribution. The top row of Fig 1 shows such a random array array chosen so that the probability per unit area of having an antenna follows r^{-2}. This distribution is obtained by selecting the azimuth of each antenna from a random uniform distribution between 0° and 360° degrees while the radius is chosen from a probability distribution per unit radius $\propto 1/r$. (The resulting array is perhaps close to what would be obtained if a bucket of golf balls were hit and an antenna placed where each ball landed - A.Beasley, private communication).

In fact the array shown in the top row of Fig 1 is the one giving the best uv coverage out of 10 different realizations. Despite this optimisation the resulting uv coverage is quite poor, with large regions with low densities of uv points. Furthermore as telescopes are moved from the outer pads to the unoccupied inner pads the zenith uv coverage will be very different. Therefore one of the main advantages of zoom arrays, that the uv coverage is scaled, does not apply very well to random arrays.

The poor performance of the random array of 48 elements should not be too surprising. It is often assumed that with >40 elements the uv coverage of the MMA/LSA is automatically guaranteed to be good whatever the telescope distribution. However between 40 and 64 elements are not in fact very many if we desire both good 2D uv coverage and to instantaneously cover a wide range of baseline lengths. For the random array given in Fig 1, with 48 elements distributed over a range of 10 in radius there will on average be only 14.5 antennas which lie in the annulus covering the outer factor of two of radius. This means that within each such annulus on average there are only $N_Q = 3.6$ antennas per quadrant in azimuth. Given statistical fluctuations of order r.m.s $\sqrt{N_Q}$ there is high probability of some such sectors being completely free of antennas.

4.3 Circular Ring Arrays

The other logical limit for a circularly-symmetric, self-similar, configuration is to distribute the antennas evenly on a regular 'dartboard' distribution. In such a distribution the antennas lie on a

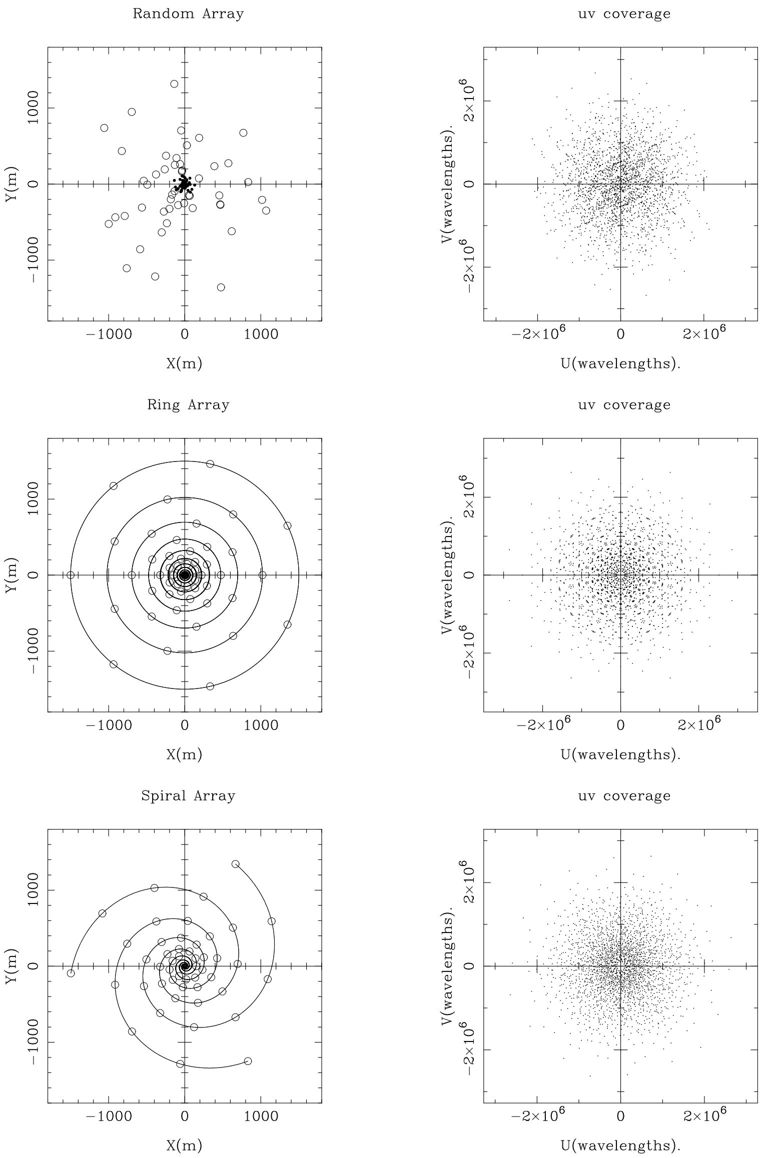

Figure 1: Three two-dimensional arrays with the same antenna density distribution but different geometries. All configurations have antennas placed over a range of 10 in radius from the array centre. Nb uv coverages are calculated assuming a wavelength of 1mm. TOP ROW - Circles show the positions of 48 antennas randomly placed according to an antenna probability distribution proportional to $1/r^2$, where r is the radius from the centre. The dots in the centre indicate the positions of unoccupied pads, to which the telescopes would be moved as the array zooms in. MIDDLE ROW-Configuration and zenith uv coverage for a regular circularly symmetric array of 49 antennas consisting of 7 antennas placed on the outer 7 rings of a self-similar concentric ring pattern. As the array zooms in antennas are moved from the outer circle to the largest unoccupied circle in the centre (see Fig 4). BOTTOM ROW - Configuration and zenith uv coverage for a 48 antenna (16 antennas per arm) regular 3-armed pattern with $\Delta\phi = 1.51$. As the array zooms in antennas are placed on unoccupied pads in the inner part of the spiral pattern (see Fig 5).

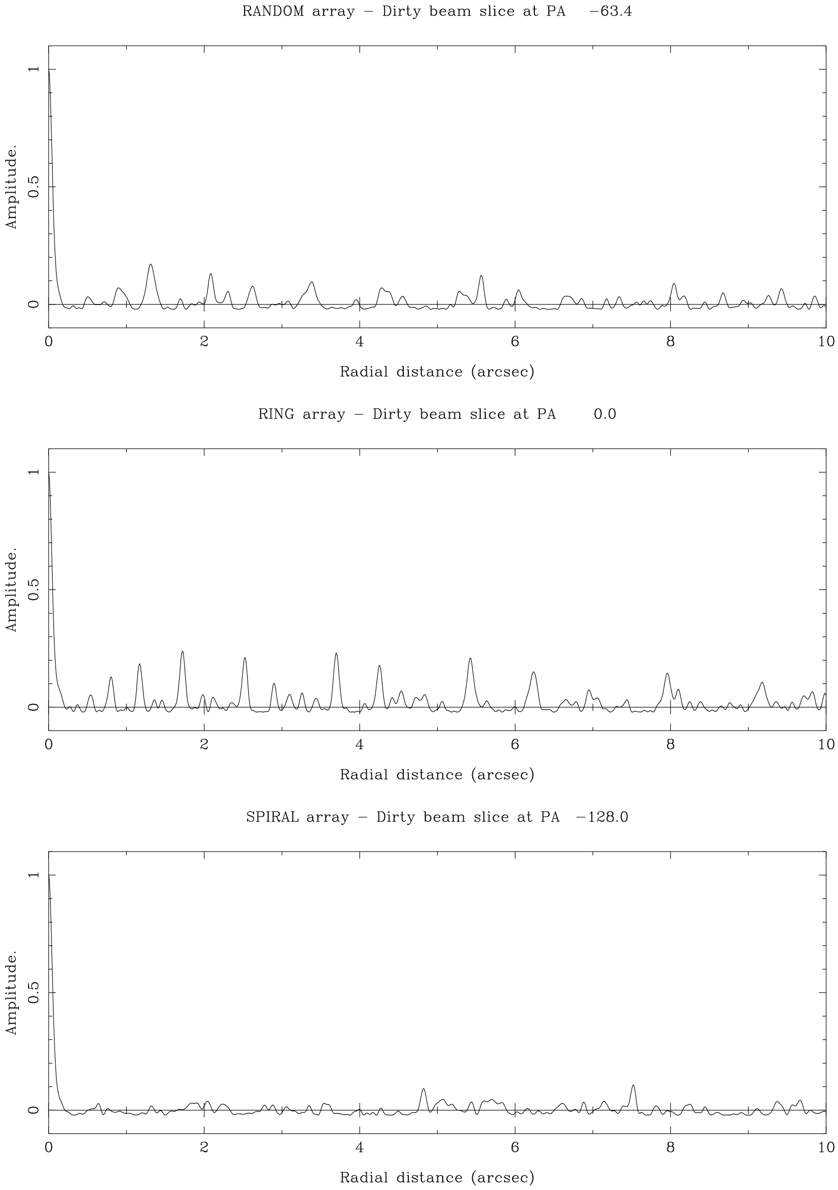

Figure 2: Slices through the naturally weighted dirty beam for each of the configurations and uv coverages shown in Fig 1. In each slice the PA is chosen to pass through the peak sidelobe found within 30 beams of the centre. TOP ROW - slice for the randomly distributed array. MIDDLE-ROW Slice for the circularly symmetric concentric ring geometry (beam FWHM = 0.088 arcsec). BOTTOM-ROW Slice for the spiral array (beam FWHM=0.108 arcsec)

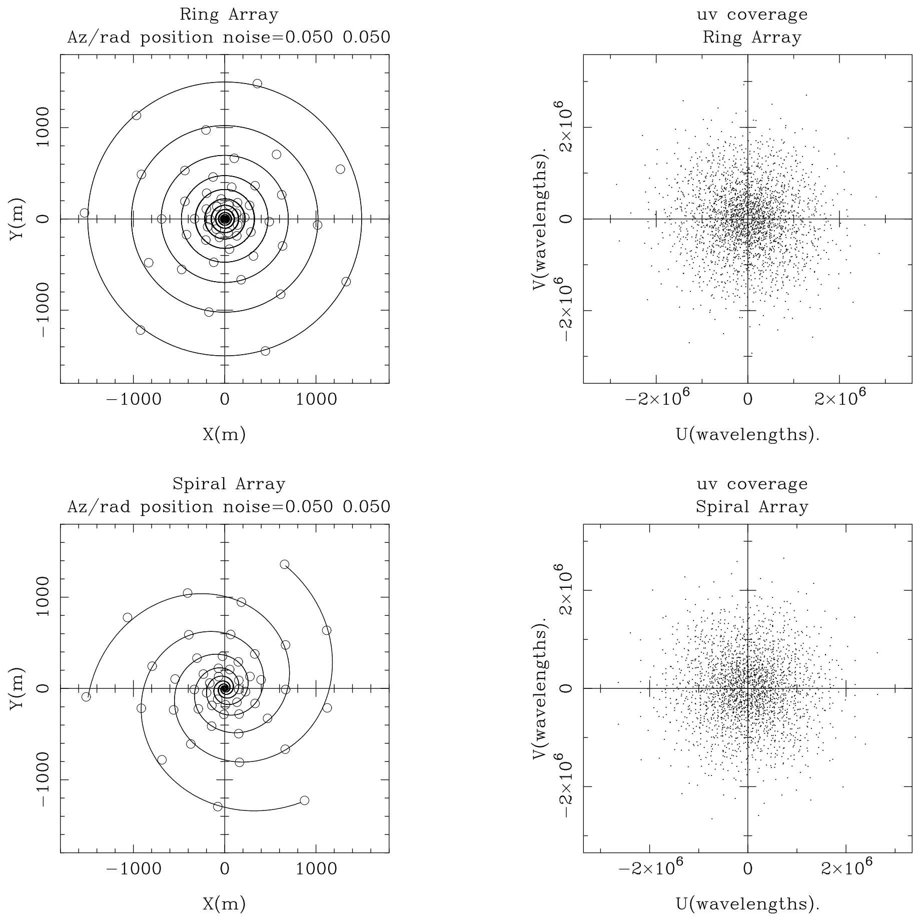

Figure 3: Effects of applying random perturbations to the antenna positions. TOP ROW - array and uv coverage for the ring array from Fig 1 after displacing the antenna positions in radius and azimuth with perturbations drawn from random gaussian distributions with r.m.s equal to 0.05 of the radius to each antenna. BOTTOM ROW - array and uv coverage for a similarly perturbed spiral array. Note that this perturbation is sufficient to remove most of the spiral artifacts but significant inhomogeneities in the ring uv coverage persist. Note also that for the case of the perturbed ring array the density of points as a function of radius has pronounced steps at 0.5 and 1.5Mλ (i.e. the 'Wedding Cake' effect).

series of concentric rings, with each ring having a constant ratio in radius to the next smallest ring (see Fig 1, middle row). If there are an equal number of antennas on each ring them the antenna density obeys $\rho(r) \propto r^{-2}$ and the array is self-similar.

In the simplest such array the N_{ant} antennas on each ring are equally spaced in azimuth by $\Delta\phi = 2\pi/N_{ant}$, and the azimuths of the antennas on each ring are the same as on the one before, giving rise to a pattern of N_{ant} spokes. If instead each ring is rotated by an angle of $\Delta\phi/2$ from the next smallest then a more uniform configuration (see Fig 1, middle row) is obtained with a better uv coverage. (If the twist between the rings is something other than 0 or $\Delta\phi/2$ then the pattern of the array is a N_{ant} armed spiral). It is also found advantageous in terms of uv coverage to choose N_{ant} to be an odd number. This is because if N_{ant} is even then uv coverage becomes doubly redundant and the effective number of uv points is halved (consider for instance the vector between two antennas, both at PA 0°, on two different rings, exactly the same vector arises between the two corresponding antennas at 180°).

Given the above arguments we show results for a regular concentric ring array with $N_{ant} = 7$ antennas per ring and $N_{ring} = 7$ rings (i.e. 49 antennas in total) and an azimuth twist of $\Delta\phi/2$ between adjacent rings (see Fig 1, middle row). The resulting uv coverage is highly geometrically regular and has large variations in the local density of uv points. Many regions of the uv plane are poorly sampled. Because of the regularity of the uv coverage it is not surprising that the naturally weighted dirty beam has many large ringlobes (see Figure 2). Other choices of numbers of rings and antennas per ring with around 48 antennas (e.g. 5 rings of 9 antennas, or 4 rings of 11 antennas) give even worse uv coverages. The uv coverages and beams of concentric ring arrays can be improved significantly by adding random perturbations on the positions of each antenna (see Section 4.5) - however we shall argue that it is better to start by perturbing a regular pattern which gives a more uniform coverage.

4.4 Spiral Array

Next we consider a regular 3-armed spiral array. Once the number of antennas (i.e. 48 or 16 per arm) and range of radii (10) have been specified then the array geometry is completely defined by the change in azimuth in going from the first antenna on each arm to the last antenna on each arm ($\Delta\phi$). We find that for a range of $\Delta\phi$ between 1.2 and 2.0 turns reasonable uv coverages are produced. However the presence of spiral artifacts in the uv coverage is found to depend quite critically on the exact value of $\Delta\phi$ chosen. By trial and error we find that $\Delta\phi = 1.51$ turns gives the most uniform coverage.

We find that the resulting uv coverage for a regular spiral is much more evenly distributed than for the regular circular ring array (see Fig 1, bottom row). The dirty beam also has excellent properties (see Fig 2, bottom row). Note that despite the fact that the 3-arm spiral configuration has triangular and not circular symmetry the resulting uv coverage is close to being circularly symmetric. This is because the outer perimeter of the spiral array is close to a curve of constant diameter, the Reuleaux Triangle (see Fig 6b) with a series of nested Reauleax triangles within. The relative uniformity of the coverage compared to that of the circular ring arrays can then be explained (Keto 1997) due to the Reuleaux Triangle being the curve of constant diameter which has minimum symmetry while the circle is the one with maximum symmetry.

4.5 Perturbed Regular Arrays

The uv coverages for both ring and spiral arrays can be improved by randomly perturbing the positions of the antennas in radius and azimuth. Fig 3 shows the effect of applying random perturbations drawn from a gaussian distribution with r.m.s in both azimuth and equal to 0.05 of the radius to each antenna. Such perturbations are able to remove virtually all of the small non-uniformities present in the regular spiral uv coverage. However because the original non-uniformities in the regular ring array coverage are much larger the random perturbations are not able to completely mask them. Increasing the size of the perturbations to r.m.s. 0.1 of the radius masks the small holes in the ring uv coverage a little more but starts to introduce larger scale asymmetries in the uv coverage. By the time the perturbations have r.m.s 0.2 of radius the uv coverage is similar to that for a random array (see Fig 1, top row) are obtained.

Fig 3 also illustrates another important difference between perturbed ring and spiral arrays. Because the former consists of a series of discrete rings the uv coverage inevitably has a tiered or 'Wedding Cake' form. In Fig 3(top right) there is a clear 'step' in the density of uv point at uv radius 1.5Mλ and another one around 0.5Mλ. No such 'steps' are found in the perturbed spiral uv coverage which has a smooth radial distribution.

5 Comparison of Scaling Properties

A second point of comparison between circular and spiral arrays is how their uv coverage scales as the array zooms in or out. Ideally the uv coverage should always be close to circularly symmetric and always be self-similar, just differing by a scale factor as the antennas are moved.

As discussed in Section 4.2 a totally random array is expected to have poor self-scaling properties. Here therefore we consider only (randomly perturbed) ring and spiral arrays. Fig 4 shows the case of the ring array. The top panel shows the array in its largest configuration in which there are seven antennas on each of the seven largest rings. As the configuration is shrunk antennas are moved from the largest ring and placed on the previously unoccupied eighth largest ring. The middle panel shows the situation when just over half of the outer 'shell' i.e. four antennas, have been moved. The bottom panel shows the case when the whole outer shell has been moved inward. Only in the first and last cases is the uv coverage circular and self-similar, with a scale ratio of 1.47 between the uv coverages. When the array is half-moved the uv coverage is significantly elongated in the SW to NE direction, giving rise to an elliptical beam.

Figure 5 shows the case of a spiral array. Again the top panel shows the largest possible configuration. The uv coverage scales almost exactly when one antenna is moved from the end of each arm to the start of each arm (bottom panel) i.e. when only three antennas are moved. The spiral has a unique 'twist-zoom' property in that after moving only three antennas the configuration just rotates and shrinks by a small factor of 1.16. Because the uv coverage of each array is close to circularly symmetric the rotation is irrelevant. The middle panel shows the case when only one antenna from one arm has been moved inward (the uv coverage is similar when a total of two antennas are moved in). In contrast to the ring arrays even when in this 'half moved' state the spiral's uv coverage is very close to circularly symmetric. The spiral therefore seems to have two inbuilt advantages over concentric ring arrays. First the number of telescopes required to move to get self-similarity (3 versus 7) and the resulting ratio of scale factors (1.16 versus 1.47) are both significantly smaller allowing us to adjust the resolution very finely. Secondly even when in its 'half-moved' state the uv coverage of the spiral is close to optimum while that of the ring array is not.

6 Infrastructure Requirements

Another way to compare the circular and spiral arrays is in terms of their infrastructure requirements. This infrastructure includes the rough 'roads' along which the antennas are moved. It also includes the total length of conduits, power cables and optic fibres linking the antennas to the central control building.

A full analysis of the infrastructure requirements of each configuration have not yet been made - but a first order comparison by comparing the total 'road' length connecting the antennas. Using this measurement it might appear that some ways of connecting ring arrays give lower road and antenna move length requirements than for spiral arrays. For instance if the antennas on the ring array in Fig 1 (middle row) were connected by 7 straight spokes - with short orthogonal branch spurs to accommodate the azimuth shift between rings, then the total road length is $9.1R_{max}$ where R_{max} is the radius of the outer ring. In contrast for the spiral array in Fig 1(bottom row) the three spiral roads have total length $11.1R_{max}$ where R_{max} is the radius out to the antenna at the end of each arm. In order to reduce the distance over which antennas must be carried during reconfiguration, which would otherwise be very long, it is advantageous to consider adding to the spiral three or four straight 'access roads' along radii (Conway 1998). If three such straight roads of length R_{max} are added then the total road length becomes $14.1R_{max}$; considerably more than for the ring array. Expressed in terms of the maximum baseline ($2R_{max}$ for the rings compared to $1.75R_{max}$ for the spiral) the advantage for the ring array is even more pronounced.

There are however alternative ways of connecting the telescopes in a spiral array which dramatically reduce the total road length and the distance over which the antennas must be moved while reconfiguring. Figure 6c shows one such method of 'wiring' a spiral, in which 9 slightly curved roads are used. In this pattern the total road length is $7.8R_{max}$ which is less than that needed to connect the regular ring array. Since the roads are almost straight the distance required to move the antennas while reconfiguring the array is also close to the minimum possible. It is important to note that individual antennas can still be thought of as belonging to one of the three spiral arms indicated in Fig 6a and when zooming the scheme outlined in Fig 5 is still used. Antennas are still moved from the ends of each of these three spiral arms to the start of same spiral arm; but they are moved along the pattern of roads shown in Figure 6c.

7 Interfacing with Compact and Extended Arrays

One final area in which to compare circular symmetric of spiral zoom array designs is how they interface with the most compact array and with larger arrays. Obviously this question depends critically on the exact design of these other arrays, but there are some general observations that can be made. For the case of the compact array in which the telescopes are placed as close as possible consistent with access and shadowing constraints, the best packing density occurs when the pads are located on a triangular lattice; it might therefore be most natural to interface to a zoom array which has natural three-fold symmetry like a three-armed spiral. However it is worth noting that there are also disadvantages to having a regular triangular lattice for the close-pack

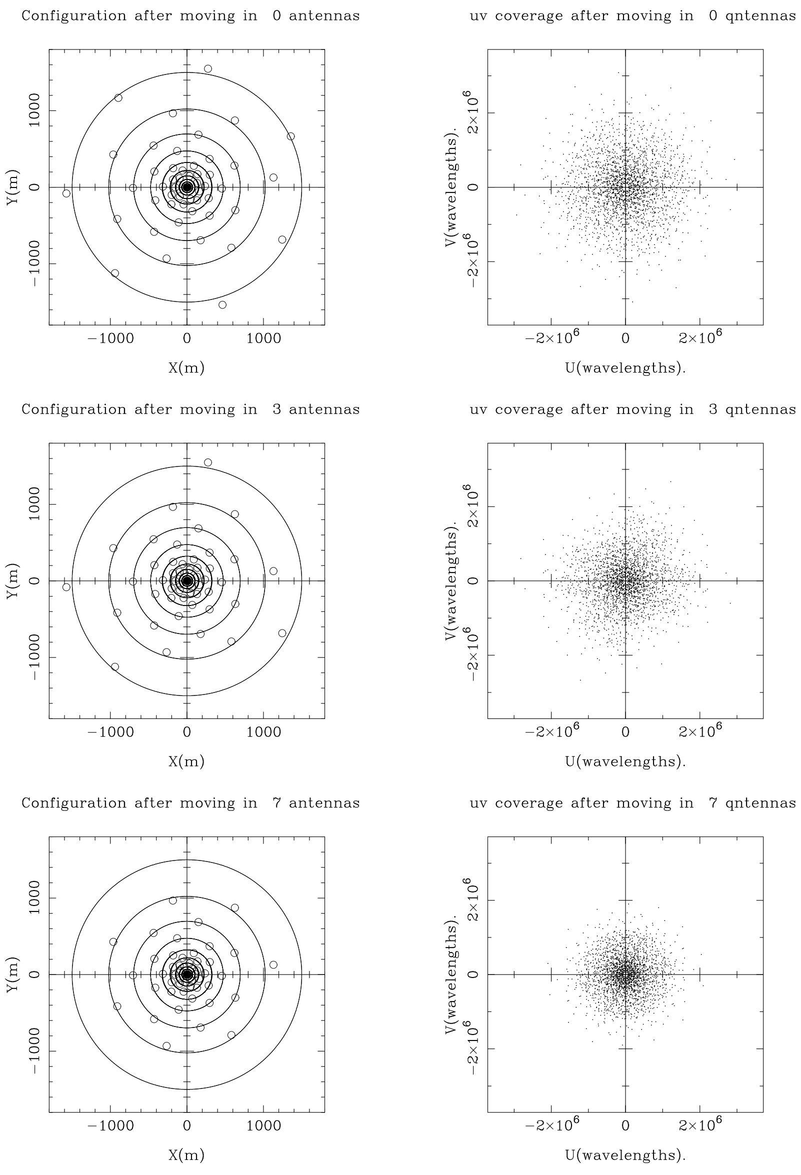

Figure 4: Concentric Ring array - Illustration of how uv coverage changes as antennas are moved inwards. TOP-ROW The largest configuration in which the outer 7 rings are each filled with 7 antennas. MIDDLE-ROW Configuration and uv coverage after moving in 3 out of 7 of the antennas to the 8th biggest ring, the uv coverage is significantly elongated giving rise to an elongated synthesised beam. BOTTOM-ROW after moving in all of the 7 antennas initially on the outer ring, the uv coverage is a scaled version of that in the original array of maximum size - except that all baselines are reduced in length by a factor of 1.47

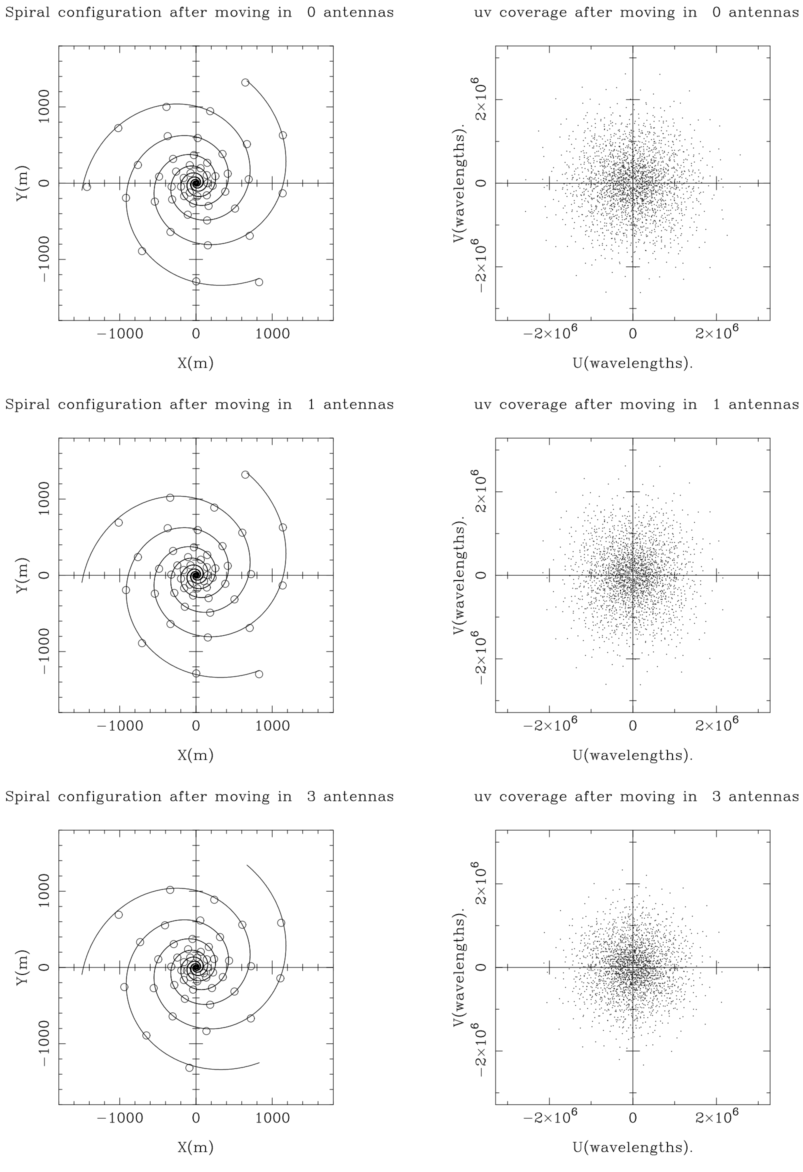

Figure 5: Spiral array - Illustration of how uv coverage changes as antennas are moved inwards. TOP-ROW The largest configuration in which the outer 16 stations on each arm are filled. MIDDLE-ROW Configuration and uv coverage after moving in the antenna on the Eastern most arm, the uv coverage remains close to circularly symmetric. BOTTOM-ROW Configuration and uv coverage after moving in a total of 3 antennas (1 per arm). The uv coverage is a scaled version of that in the original array of maximum size (top row) - except that all baselines are reduced in length by a factor of 1.16

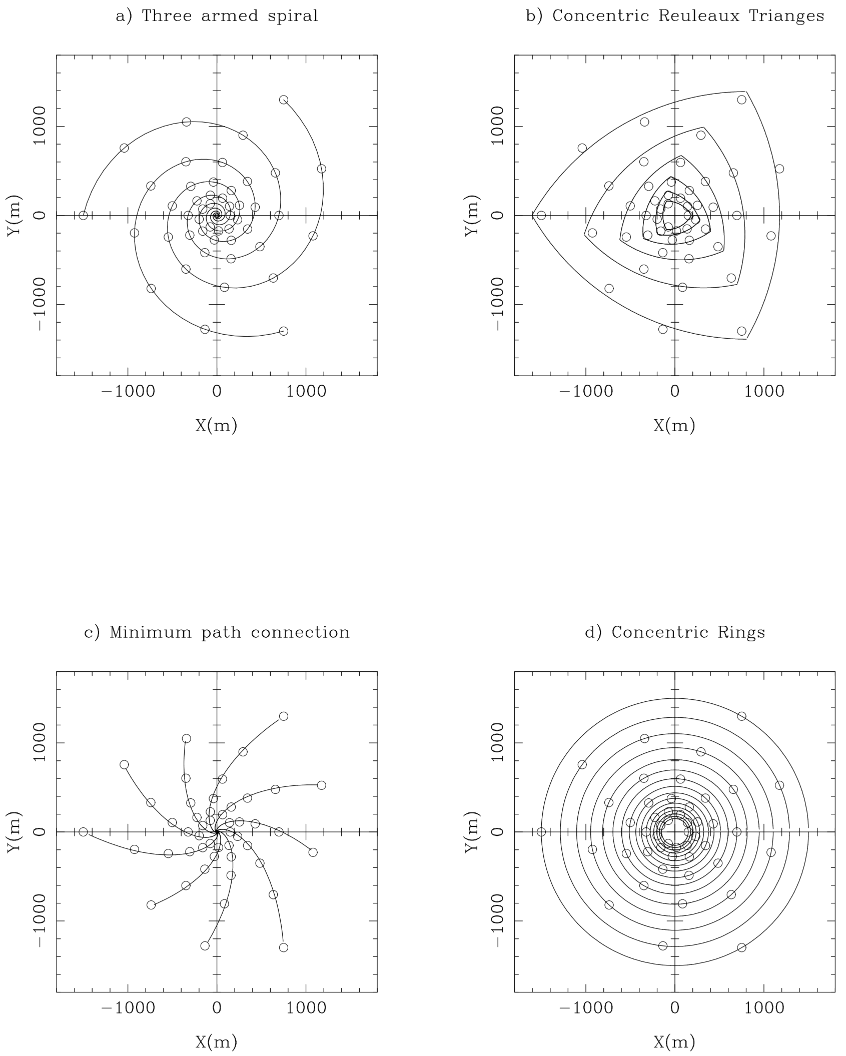

Figure 6: Four ways of viewing the same spiral distribution of antennas. a) As antennas on a three-armed spiral pattern. b) Approximately as a set of nested Reuleaux triangles. c) As a nine-armed spiral with arms of unequal length to give a triangular outer boundary. This pattern minimises the road construction and distance each antenna must be carried - and is therefore the optimum choice for the road and conduit geometry for such an array. d) As a nested set of circles with three antennas per circle and a small azimuth rotation between each circle.

array. For such a pattern baseline redundancy is high and the sidelobe levels will be large. A possible alternative which should be considered, which has almost the same packing density but much less regularity, is a quasi-crystalline pattern based on Penrose or other quasi-periodic tilings (see Gardner et al 1977).

At the other extreme there is the question of the interface with the 10km array and ring-like array of 3km diameter. The path of the 10km array is dictated by terrain constraints and must be a closed loop enclosing a hilly region of the site. This array can be smoothly interfaced to a spiral by simply extending the Northernmost and Southernmost of the arms shown in Figure 6c and forming a closed loop of diameter 10km. As explained in Conway (1998) in order not to have a serious gap in resolution between the largest zoom array filling the 3km plain and the 10km array it is necessary to consider a 'ring-like' 3km diameter array. There may be advantages as claimed by Keto(1997) to having such arrays based on Reuleaux triangles rather than circles. As shown in Fig 6b the spiral zoom array can be considered as a set of nested Reuleaux triangles and therefore can naturally interface to such a ring while minimising the number of new pads and access roads that must be built. For instance we could move from the largest spiral zoom array to a 'fat ring' Reauleux triangle by retaining antennas on the outer three nested triangles shown in Figure 6b and distributing the remaining antennas at new pad positions scattered between the largest (outer) and the third largest Reuleaux triangles.

8 Conclusions

We have carried out a first comparison of zoom arrays with circular and three armed spiral symmetry. For circular arrays of a limited number of antennas it has been demonstrated how important is the exact two dimensional distribution of antennas in determining the uv coverage and beam shape. This shows that although useful for quickly exploring parameter space, we must be cautious in drawing conclusions from analytic models based on smooth antenna density distributions and one-dimensional Hankel transforms (e.g. Webster 1998,1999). Our results are effected perhaps by the fact that the optimum method of 'tiling' a circular region have not been found. As shown in Section 4.2 a completely random antenna distribution leads to large holes in the in uv coverage. In contrast a nested ring or dartboard pattern (Section 4.3) has too much symmetry; which also gives uneven uv coverage. These effects can be reduced somewhat by randomly perturbing the antenna positions of the regular ring array but it must be possible to start with a pattern with better uv coverage properties. Perhaps such a pattern could be based on some quasi-periodic lattice (see Gardner et al 1977) as was also discussed in Section 7 in the context of the optimum close-pack array.

With the above proviso our simulations so far do seem to indicate that spiral zoom arrays have some small but significant advantages in both uv coverage and scaling properties. These advantages seem to be related directly to the three-armed spiral geometry. From the point of view of uv coverage it appears that the advantages of three-fold symmetry discussed by Keto (1997) for ring-like arrays also apply to filled arrays. In terms of scaling properties the fact that the spiral is an 'open' pattern with a unique 'twist-zoom' property gives it an advantage in how finely the array resolution can be adjusted and how self-similar the coverage remains as antennas are moved.

Despite the small advantages we find for spiral over circular symmetric zoom arrays it is important to note that either type would give significant advantages over the series of set configurations that has been favoured to date. The peak sidelobe level of the zoom arrays discussed in this memo (which is probably a very imperfect measure of imaging quality; see the discussion in Sect 4.1) are only slightly larger, e.g 0.10 for the regular spiral in Fig 3, than those expected for fixed array geometries with minimised sidelobes (see e.g. Kogan 1998); yet there are are great additional advantages to zoom arrays. These advantages include continuously adjustable resolution and reduced numbers of pads and roads. We believe zoom designs should be seriously considered for the intermediate arrays of the LSA/MMA.

References

Conway, J.E., 1998, MMA Memo 216.
Gardner. M., 1977, Scientific American, Vol 236, p 110.
Keto, E., 1997, ApJ 475, 843.
Kogan, L., 1998, MMA Memo 226.
Kogan, L., 1999, MMA Memo 247.
Viallefond, 1998, LSA/MMA Feasibilty Study, April 1998, Sect 3.5
Webster, A., 1999, MMA Memo 239.
Webster, A., 1999, MMA Memo 233.